

Biological Chemistry ‘Just Accepted’ Papers

Biological Chemistry ‘Just Accepted’ Papers are papers published online, in advance of appearing in the print journal. They have been peer-reviewed, accepted and are online published in manuscript form, but have not been copy edited, typeset, or proofread. Copy editing may lead to small differences between the Just Accepted version and the final version. There may also be differences in the quality of the graphics. When papers do appear in print, they will be removed from this feature and grouped with other papers in an issue.

Biol Chem ‘Just Accepted’ Papers are citable; the online publication date is indicated on the Table of Contents page, and the article’s Digital Object Identifier (DOI), a unique identifier for intellectual property in the digital environment (e.g., 10.1515/hsz-2011-xxxx), is shown at the top margin of the title page. Once an article is published as **Biol Chem ‘Just Accepted’ Paper** (and before it is published in its final form), it should be cited in other articles by indicating author list, title and DOI.

After a paper is published in **Biol Chem ‘Just Accepted’ Paper** form, it proceeds through the normal production process, which includes copy editing, typesetting and proofreading. The edited paper is then published in its final form in a regular print and online issue of **Biol Chem**. At this time, the **Biol Chem ‘Just Accepted’ Paper** version is replaced on the journal Web site by the final version of the paper with the same DOI as the **Biol Chem ‘Just Accepted’ Paper version**.

Disclaimer

Biol Chem ‘Just Accepted’ Papers have undergone the complete peer-review process. However, none of the additional editorial preparation, which includes copy editing, typesetting and proofreading, has been performed. Therefore, there may be errors in articles published as **Biol Chem ‘Just Accepted’ Papers** that will be corrected in the final print and online version of the Journal. Any use of these articles is subject to the explicit understanding that the papers have not yet gone through the full quality control process prior to advanced publication.

Research Article

**An alternative processing pathway of APP
reveals two distinct cleavage modes
for rhomboid protease RHBDL4**

Sherilyn Junelle Recinto^{1,2}, Sandra Paschkowsky¹ and Lisa Marie Munter^{1,*}

¹McGill University, Department of Pharmacology and Therapeutics and Cell Information Systems group, Bellini Life Sciences Complex, 3649 Sir-William-Osler Promenade, Montreal H3G 0B1, Quebec, Canada

²Integrated Program in Neuroscience, McGill University, Montreal H3A 2B4, Quebec, Canada

*Corresponding author

e-mail: lisa.munter@mcgill.ca

Abstract

Since the first genetic description of a rhomboid in *Drosophila melanogaster*, tremendous efforts were geared towards elucidating the proteolytic mechanism of this particular class of intramembrane proteases. In particular, mammalian rhomboid proteases sparked our interest and we aimed to investigate the human homologue RHBDL4. In light of our recent finding of the amyloid precursor protein (APP) family as efficient substrates of RHBDL4, we were enticed to further study the specific proteolytic mechanism of this enzyme by comparing cleavage patterns of wild type APP and APP TMS chimeras. Here, we demonstrate that the introduction of positively charged amino acid residues in the TMS redirects the RHBDL4-mediated cleavage of APP from its ectodomain closer towards the TMS, possibly inducing an ER-associated degradation (ERAD) of the substrate. In addition, we concluded that the cytoplasmic tail and proposed palmitoylation sites in the ectodomain of APP are not essential for the RHBDL4-mediated APP processing. In summary, our previously identified APP ectodomain cleavages by RHBDL4 are a subsidiary mechanism to the proposed RHBDL4-mediated ERAD of substrates likely through a single cleavage near or within the TMS.

Keywords: endoplasmic reticulum-associated degradation (ERAD); rhomboid protease; Alzheimer's disease; intramembrane protease; cleavage mode

Introduction

Rhomboid proteases are an ancient class of intramembrane serine proteases that is highly conserved throughout all kingdoms of life (Kinch *et al.*, 2013; Lemberg *et al.*, 2007a). Among the 14 mammalian rhomboid family members are five proteases that contain a catalytically active serine-histidine dyad (Urban *et al.*, 2001; Wang *et al.*, 2006). Although the physiological functions of these proteolytically active rhomboids are still poorly understood, their recent implications in various diseases substantiate the quest for their physiological substrates. Human mitochondrial presenilin-associated rhomboid-like protein (PARL) has been associated with Parkinson's disease (Shi *et al.*, 2011) and type II diabetes (Walder *et al.*, 2005), while endoplasmic reticulum (ER)-resident rhomboid-like protein 4 (RHBDL4) has been linked to colorectal cancer (Miao *et al.*, 2017; Song *et al.*, 2015), glioblastoma (Stangeland *et al.*, 2015) and a particular sensory-motor neuropathy (Fleig *et al.*, 2012). In the pursuit of identifying substrates for human rhomboids, our group found that RHBDL4 efficiently cleaves the amyloid precursor protein (APP), a key player in Alzheimer's disease pathogenesis. We demonstrated an alternative, non-amyloidogenic APP processing pathway leading to the emergence of specific RHBDL4-derived N-terminal and C-terminal fragments (Paschkowsky *et al.*, 2016). Knockdown of RHBDL4 in HEK 293T cells diminished endogenous APP cleavage fragments indicating that RHBDL4 and APP constitute a physiologically relevant enzyme-substrate pair. Furthermore, all cleavages identified so far are thought to be within the APP ectodomain, thereby prompting us to further investigate this intriguing cleavage mechanism. An earlier study by Fleig and colleagues postulated the relevance of RHBDL4 in the degradation of predestined type I or multi-pass transmembrane proteins in the ER as well as implicated the ubiquitin interacting motif present in the C-terminal domain of RHBDL4 in this degradation pathway (Fleig *et al.*, 2012). As such, we exploited these previous findings which identified RHBDL4 substrates (MPZ-L170R) and non-substrates (MPZ), and generated different APP chimeric constructs, substituting the APP TMS with the TMS of either MPZ-L170R or MPZ. Furthermore, we studied the impact of the APP C-terminal domain on RHBDL4-mediated APP processing as well as the influence of a proposed back folding of the APP ectodomain to the membrane induced by palmitoylation at specific cysteines residues (Bhattacharyya *et al.*, 2013). Here we show that RHBDL4 may have two distinct cleavage modes: predominating cleavage in the TMS or in the juxtamembrane region, which possibly depends on the composition of the substrate

transmembrane sequence and a second mode where APP gets cleaved multiple times in its ectodomain, potentially induced by specific environmental settings.

Results

Membrane-bound substrates of RHBDL4 can undergo two distinct proteolytic cleavage modes

Rhomboid proteases have been originally described as intramembrane proteases, thus they are assumed to predominantly cleave their substrates in the transmembrane sequence (TMS) (Lemberg *et al.*, 2007b). However, we recently identified the human rhomboid protease RHBDL4 and APP as enzyme-substrate pair and showed that RHBDL4 cleaves APP multiple times in its ectodomain (Paschkowsky *et al.*, 2016). These cleavages generate 70-73 kDa N-terminal fragments (NTFs) and 10-25 kDa C-terminal fragments (CTFs) (Paschkowsky *et al.*, 2016). This rather unexpected finding challenged us to further investigate the specific substrate recognition mechanism of RHBDL4 for APP. As such, we aimed to analyse RHBDL4-mediated processing of different APP TMS mutants. Previously, RHBDL4 was demonstrated to process membrane-bound proteins encompassing TMS predestined for endoplasmic reticulum-associated degradation (ERAD) (Fleig *et al.*, 2012). We took advantage of these proposed substrates to generate APP mutants wherein the TMS of wild type APP was exchanged for the TMS of a proposed RHBDL4 substrate or non-substrate (Figure 1A). In this regard, we mainly focused on myelin protein zero (MPZ), which is a key player in myelination of peripheral neurons (Marrosu *et al.*, 1998). A single amino acid exchange from leucine to arginine in the TMS of MPZ, namely MPZ L170R, induces a genetic predisposition to Charcot-Marie-Tooth disease, a hereditary sensory and motor neuropathy (Numakura *et al.*, 2002). Contrary to wild type MPZ, the variant was shown to be cleaved by RHBDL4. We thus analysed the processing of APP containing either the MPZ TMS or MPZ L170R TMS variant by RHBDL4.

In accordance with our previous report (Paschkowsky *et al.*, 2016), co-expression of wild type APP with active RHBDL4 in comparison to inactive led to a decrease in full-length APP and a concomitant increase in 70-73 kDa NTFs (Figure 1B). Similar results were obtained upon co-expression of RHBDL4 with different APP TMS mutants; production of the 70-73 kDa NTFs was observed for all mutants (Figure 1B). However, cleavage of APP-MPZ L170R

generated an additional, larger fragment running around 90 kDa, in very close proximity to immature full length APP (indicated by a red arrow). This suggests the occurrence of an additional cleavage site for this mutant as compared to APP WT. We then proceeded to evaluate the CTFs pattern. Surprisingly, cleavage of APP-MPZ, but not APP-MPZ L170R, resulted in RHBDL4-specific CTFs in the range of 15-27 kDa similar to the wild type [note that these fragments migrate slightly higher than those described in Paschkowsky *et al.* (2016), due to the C-terminal flag tag, Figure 1C]. Interestingly, APP MPZ L170R cleavage generated a fragment smaller than the thus far described, at approximately 12 kDa (indicated with red arrows in Figure 1C). We also observed that the staining of APP CTFs derived from APP-MPZ cleavage was more pronounced upon active RHBDL4 co-expression in comparison with wild type APP. This suggests that APP-MPZ might be a better substrate for RHBDL4, which is further supported by the occurrence of APP CTFs upon co-expression with RHBDL4 inactive, implying that these fragments are derived from endogenous RHBDL4 activity. We formerly concluded, based on antibody-dependent epitope mapping, that the smallest wild type APP CTF derives from a cleavage between the cleavage sites of α - and β -secretase (Paschkowsky *et al.*, 2016). Considering the apparent molecular weight of the newly generated small fragment of APP-MPZ L170R, RHBDL4 possibly cleaves this mutant within its TMS.

Furthermore, to investigate the relevance of the cytoplasmic APP domain, which was described to possess ubiquitination sites (El Ayadi *et al.*, 2012), for substrate recognition by RHBDL4, we also generated an APP mutant that lacks the C-terminal domain (APP Δ CTD), but should still be anchored to the membrane (Figure 1A). Co-expression with active RHBDL4 showed a decrease in full length APP Δ CTD together with corresponding occurrence of NTFs similar to wild type APP (Figure 1B). Thus, our results revealed that the APP cytoplasmic tail, and therefore potential ubiquitination of APP, is not required for RHBDL4-mediated APP ectodomain processing. APP-MPZ and APP Δ CTD mutants are recognized and cleaved by RHBDL4 in the ectodomain; however, substitution with the TMS of MPZ L170R altered the cleavage mechanism of RHBDL4, instigating the formation of novel NTFs and CTFs.

Single amino acid substitution in the APP TMS circumvents initial cleavages in the ectodomain by RHBDL4

The differences in cleavage pattern observed between APP-MPZ and APP-MPZ L170R pertains to the subsequent question as to what drives the change in RHBDL4 processivity. Fleig *et al.* (2012) demonstrated that the presence of two positively charged amino acid residues in the TMS promotes RHBDL4-mediated ERAD of the membrane-bound substrate, possibly through destabilization of the helix embedded within the lipid bilayer. Consequently, we generated an APP transmembrane point mutant, substituting the valine at position 640 with an arginine (APP V640R) and thereby mimicking the position of the arginine residue in the MPZ variant L170R (Figure 1A). We hypothesize that APP V640R is degraded in the ER by RHBDL4 through a single cleavage near or within the TMS as opposed to the previously described, multiple RHBDL4 cleavages in the APP ectodomain. As expected, we observed the 70-73 kDa NTFs for APP V640R, but interestingly, we also detected an additional, novel NTF fragment at approximately 90 kDa similarly to MPZ L170R (indicated by red arrow in Figure 2A). Detection of the corresponding CTFs of APP V640R revealed that RHBDL4-specific fragments as seen for wild type APP were absent in this variant. However, a small fragment at approximately 12 kDa migrating at the same molecular weight as the upper small CTF from APP-MPZ L170R was detected in lysates from cells co-expressing the active but not inactive RHBDL4 (indicated by the upper red arrow in Figure 2B). The absence of the large RHBDL4-mediated APP CTFs for the V640R variant suggests that either the RHBDL4 cleavage pattern was altered or the mutation affects the overall stability of these CTFs, which may lead to faster degradation. To test if potential large CTFs from APP V640R were quickly degraded by the proteasome, cells were treated with the proteasomal inhibitor MG132. As shown in Figure 2C, the treatment enhanced the levels of induced myeloid leukemia cell differentiation protein 1 (Mcl-1), suggesting inhibition of the proteasomal degradation pathway. However, no enrichment in RHBDL4-specific 15-27 kDa CTFs was observed in cells expressing the APP variants. Hence, APP V640R and APP-MPZ L170R variants are likely processed differently by RHBDL4 compared to wild type APP. Strikingly, we observed elevated levels of the small CTFs derived from the APP V640R and APP-MPZ L170R variants upon MG132 treatment (indicated by the upper red arrow), suggesting proteasomal degradation for these fragments. Notably, the smallest CTF detected in lysates of cells overexpressing wild type APP with either active or inactive RHBDL4 (indicated by the pink arrow in Fig 2B-D), possibly generated from γ -secretase cleavage within APP TMS (Wolfe,

2012), ran about the same molecular weight as the novel fragment from APP V640R and APP-MPZ L170R cleavages (Figure 2B-D). We therefore tested whether γ -secretase activity is required in the generation of the observed novel fragment. As expected, γ -secretase inhibition enhanced the signals for α/β -CTF (indicated by yellow arrow in Figure 2D). However, the 12 kDa fragment of either APP mutants was not affected by γ -secretase inhibition indicating that they are indeed derived from RHBDL4 activity (Figure 2D). Please note that we observed faint signals for APP CTFs upon co-expression of wild type APP with inactive RHBDL4, suggesting that they are derived from endogenous RHBDL4 activity. This, however, was not the case for the APP mutants (Figure 2D) implying that the two cleavage modes apply not only to overexpressed RHBDL4, but also endogenous RHBDL4. Consequently, the exchange of a single amino acid in the TMS of the RHBDL4 substrate APP seemingly triggers a change in the RHBDL4 cleavage mode. While wild type APP and APP-MPZ may predominantly be cleaved in their ectodomains generating large C-terminal fragments, APP V640R or APP MPZ L170R may redirect the RHBDL4 cleavage site towards the juxtamembrane region/TMS, precluding initial ectodomain cleavages.

Cysteine residues possibly implicated in the APP ectodomain back folding to the membrane are not required for RHBDL4-mediated processing

The RHBDL4-mediated APP ectodomain cleavages between the TMS and E2 domain (Figure 1A) suggest that this region must gain access to the active center of RHBDL4 through a still unknown mechanism (Paschkowsky *et al.*, 2016). Notably, the structure of the E2 domain was solved, but no structure was determined thus far for the linker region between E2 and the TMS. We therefore hypothesized that the proposed flexibility of this linker region would facilitate a close proximity of the APP ectodomain to the membrane surface, for instance, by back folding (Kaden *et al.*, 2012; Reinhard *et al.*, 2005). Interestingly, the notion of back folding has been studied in APP wherein the ectodomain has been described to anchor to the membrane upon palmitoylation of two critical cysteines (C186 and 187) in the ectodomain (Bhattacharyya *et al.*, 2013). As such, we exchanged the cysteine residues to alanine (C186-187A) to potentially abolish palmitoylation at these sites, and consequently, we anticipated cleavage abrogation if back folding through these cysteine residues would be important (Figure 1A). However, the APP variant C186-187A was processed similarly as the wild type APP based on NTF as well as CTF generation suggesting that those ectodomain cysteine residues may not play a major role in RHBDL4-mediated APP processing (Figure 3A, B).

Discussion

While bacterial rhomboid homologues were the first intramembrane proteases to be crystallised (Wang *et al.*, 2006), research on mammalian rhomboid proteases is still at its infancy. Nevertheless, several research groups, including ours, recently elucidated potential physiological functions of several human homologues by identifying novel substrates and further linking them to diseases (Adrain *et al.*, 2012; Cheng *et al.*, 2014; Christova *et al.*, 2013; Johnson *et al.*, 2017; McIlwain *et al.*, 2012; Paschkowsky *et al.*, 2016; Shi *et al.*, 2011; Song *et al.*, 2015). The description of RHBDL4-mediated APP processing as a novel APP processing pathway does not only potentially link rhomboid proteases to Alzheimer's disease, but could also shed light on the elusive physiological functions of APP (Muller *et al.*, 2017; Paschkowsky *et al.*, 2016). Using antibody-based epitope mapping, we previously concluded that RHBDL4-mediated cleavages predominantly occur in the APP ectodomain, a rather unexpected result, considering that intramembrane proteases have the unique ability to cleave membrane proteins within their transmembrane helices. It is, however, noteworthy to highlight that a crystal structure of a bacterial rhomboid displayed an active site exposed to the lumen and cleavage can take place outside of the transmembrane domain depending on the position of the substrate recognition motif (Wang *et al.*, 2006; Strisovsky *et al.*, 2009). Consequently, we sought to unravel the mechanism as to how RHBDL4 cleaves APP. In this regard, it is important to note that a previous publication implicated RHBDL4 in ERAD (Fleig *et al.*, 2012), alluding to the importance of the ubiquitin interacting motif of RHBDL4 and the acquisition of helix destabilizing residues in the substrate TMS as prerequisites for RHBDL4-mediated ERAD substrate recognition.

Intrigued by this data, we generated a chimeric APP construct containing the TMS of a proposed RHBDL4 substrate (APP-MPZ L170R), assuming that RHBDL4-mediated APP processing would still take place, or containing a TMS that does not undergo RHBDL4-mediated ERAD (APP-MPZ), anticipating that RHBDL4 would not cleave this APP chimera. Unexpectedly, however, we observed two potentially distinct cleavage modes of RHBDL4: APP-MPZ was processed similar to wild type APP in the ectodomain while APP-MPZ L170R showed generation of NTFs, but absence of previously reported RHBDL4-specific APP CTFs. Interestingly, APP-MPZ L170R generated two smaller CTFs distinct from the previous APP CTFs reported. Based on the size of the smallest fragment as well as the evident lack of the 6E10 epitope, we propose that RHBDL4 initially cleaves in very close proximity to or

within the transmembrane domain of this mutant and subsequently cleaves the soluble ectodomain to generate the 70-73 kDa NTFs. Fleig *et al.* (2012) demonstrated that the CMT disease-associated leucine to arginine mutation in the MPZ TMS induces RHBDL4-mediated ERAD of the protein, whereas the wild type form of MPZ is not cleaved nor processed through ERAD by RHBDL4. Hence, it is possible that RHBDL4 preferentially processes its substrate by cleaving within the TMS, similar to other intramembrane proteases, and solely specific conditions would trigger ectodomain cleavages. Accordingly, APP processing by RHBDL4 is perhaps subsidiary, occurring depending on the availability of unsaturated enzyme or in a disease setting. It is therefore enticing to decipher the key driver of the RHBDL4-APP processing pathway. Moreover, it will be intriguing to investigate for possibly naturally occurring variants that result from mutations in the TMS of APP, rendering the APP TMS a prime substrate for RHBDL4.

The differences in cleavage pattern observed between the APP variants, APP-MPZ and MPZ L170R, may be attributed to certain characteristics of the amino acids encompassing the transmembrane domain. Fleig and coworkers proposed that the occurrence of at least two basic amino acids (e.g. arginine and lysine, also termed “degron” motif) in the transmembrane domain could increase the susceptibility of the membrane-bound substrate for RHBDL4-triggered turnover in the ER, perhaps due to helix-destabilizing effects of these amino acids (Bonifacino *et al.*, 1990; Fleig *et al.*, 2012). Although, our knowledge regarding mammalian rhomboid proteases and their substrates is limited to date, their bacterial homologues have been crystallized and well-characterized (Arutyunova *et al.*, 2014; Lemieux *et al.*, 2007; Strisovsky *et al.*, 2014; Strisovsky *et al.*, 2009; Urban *et al.*, 2008; Wang *et al.*, 2006). These known bacterial rhomboids were shown to cleave non-physiological substrates containing helix-destabilizing residues wherein mutations reduced the processing efficiency of the enzyme (Strisovsky *et al.*, 2009). Considering the structural similarity between bacterial rhomboids and RHBDL4 (Lemberg *et al.*, 2007c), their substrate recognition mechanisms likely intersect. For GlpG, a two-stage catalytic mechanism was proposed: TMS 2 and 5 form an exosite, which retains the substrate with a partially unfolded TMS and therefore increases the likelihood of transfer to the scissile complex (Strisovsky, 2016). As such, we substituted the APP valine at position 640 to an arginine, mimicking the mutation L170R in MPZ to potentially destabilize the APP TMS in a similar manner. Strikingly, the previously described CTFs derived from ectodomain cleavages were abolished, similar to what we had observed for APP-MPZ L170R. In addition, we again detected 70-73 kDa large NTFs and one smaller

CTF, which was enriched upon MG132 treatment. We therefore suspect that these APP variants containing a “degron” motif are rapidly degraded by the proteasome, likely via RHBDL4-mediated ERAD. Furthermore, our findings contribute to the general idea that unstable helical substrate transmembrane regions are a pivotal instigator of rhomboid protease cleavage (Fleig *et al.*, 2012; Strisovsky *et al.*, 2009; Urban *et al.*, 2003). Alternatively, arginine residues were proposed to stabilize TMS sequences and it is possible that APP V640R interacts more tightly with RHBDL4 prompting its cleavage within or near the membrane. The burial of a ~~negatively~~-charged arginine residue may reduce the energy cost of membrane insertion by snorkeling the side chain into the headgroup region of the membrane and by local deformation of the lipid bilayer (Ulmschneider *et al.*, 2017). However, Ulmschneider and colleagues also suggest that due to its membrane composition, the membrane fluidity of the ER (where the RHBDL4-mediated processing takes place) may be decreased. As a result, it might not be able to accommodate the burial of an arginine, which may ultimately increase the energy cost. Consequently, the interaction between RHBDL4 and arginine-containing APP variants in the ER membrane may not necessarily be more favorable than wild type APP. Thus, a stabilized TMS is less likely to be the reason why RHBDL4 preferentially cleaves within or near the TMS of these variants as opposed to the ectodomain of wild type APP.

We also hypothesize that the dual cleavage mode of RHBDL4 may give further insight to a potential physiological role of this enzyme. It was previously shown that rhomboid pseudo-protease, iRhom2 is important in guiding TACE out of the ER (Adrain *et al.*, 2012; Christova *et al.*, 2013; McIlwain *et al.*, 2012). Similarly, RHBDL4 might modulate the ER exit of protein, in particular APP, a concept that previously has been proposed for RHBDL4 (Wunderle *et al.*, 2016). In this regard, turnover of immature, misfolded APP could be promoted by specific conditions. We have evidence that the membrane composition might impact on RHBDL4 activity, specifically membrane cholesterol (Paschkowsky *et al.*, unpublished data). This could be in line with various observations that the membrane lipid composition can confer activity and specificity to intramembrane proteases (Paschkowsky *et al.*, 2017).

Lastly, we investigated whether specific domains in APP mediate substrate recognition and affect enzyme processivity. The cytoplasmic tail of APP (APP Δ CTD) has multiple protein-protein interaction domains and is thought to bridge interacting proteins (De Strooper *et al.*, 2000; Minopoli *et al.*, 2001). Furthermore, polyubiquitination of the intracellular domain was

demonstrated to be important in regulating APP trafficking to the plasma membrane (El Ayadi *et al.*, 2012). Our findings, however, revealed that the C-terminal domain is not necessary for RHBDL4-mediated APP processing as the levels of mature C-terminally truncated APP diminished upon co-expression with the active protease and similarly, RHBDL4-derived NTFs were detected. Notably, we did not observe the occurrence of CTFs as they are likely too small to be detected in our gel system. Likewise, we demonstrated that RHBDL4-mediated APP processing does not require cysteine residues at position 186 and 187 that were previously reported to induce back folding through palmitoylation, allowing anchoring of the APP ectodomain to the membrane (Bhattacharyya *et al.*, 2013). Please note that other possible posttranslational modifications that could induce such folding were not exploited in this study. However, based on our present findings, back folding of the APP ectodomain to the membrane is a rather unlikely explanation as to how RHBDL4 cleaves APP within its linker region. Nevertheless, another idea arose: RHBDL4 could have a higher propensity to interact with unstructured, highly flexible regions that mediate ectodomain cleavages. Ultimately, this would suggest a potential chaperone-like activity of RHBDL4 similar to Derlins or iRhoms (Adrain *et al.*, 2012; Christova *et al.*, 2013; Lemberg *et al.*, 2016).

Conclusion

In our present study, we demonstrated that RHBDL4 exhibits two distinct cleavage modes that are potentially distinguished based on the composition of the substrate transmembrane sequence. Elucidating the proteolytic mechanisms of RHBDL4 could provide insight into its regulatory mechanisms, which could be exploited for novel therapeutic approaches, especially with regard to the implications of RHBDL4 in various diseases.

Materials and methods

DNA constructs

Plasmid pCMV6 containing cDNA encoding for human RHBDL4 with a C-terminal myc and flag tag was obtained from OriGene, USA. Inactive RHBDL4 S144A was generated by site directed mutagenesis using the forward primer 5'-GCT GTA GGT TTC GCA GGA GTT

TTG TTT-³ and reverse primer 5'-AAA CAA AAC TCC TGC GAA ACC TAC AGC-³. APP695 in pcDNA3.1 (Invitrogen) was provided as a kind gift of Dr. Claus Pietrzik, Johannes Gutenberg University, Mainz, Germany, and was tagged at the N-terminus with myc and at the C terminus with flag tag, which served as a template for all APP mutants described. APP mutants were cloned using gene blocks purchased from IDT. Gene blocks were dissolved in H₂O at a concentration of 10 ng/μl of which 4 ng/μl were used in a restriction enzymatic reaction with EcoRI and XbaI, at 37°C for 16-18 h. Enzymes were subsequently heat inactivated at 65°C for 20 min and stored at -20°C for later use. Simultaneously, 1 μg of pcDNA3.1 N-myc APP695 C-flag plasmid was digested by the same restriction enzymes at 37°C for 60 min followed by alkaline phosphatase treatment to avoid re-ligation of the vector, heat inactivation and purification from gels. 50 ng of vector were ligated in different ratios with digested gene blocks using T4 DNA ligase (NEB) at room temperature overnight (16-18 h). After transformation into Top10 cells via heat shock, cells were plated and incubated overnight at 37°C. DNA constructs of single colonies were then purified (Qiagen) and full sequences confirmed using DNA sequencing by Genome Quebec.

Cell culture and transfection

HEK293T cells, passaged at 80-90% confluency, were used for all transient transfections. Cells were cultured in Dulbecco's modified Eagle medium (DMEM) containing 4.5 g/l glucose, 0.584 g/l L-glutamine and 0.11 g/l sodium pyruvate (Wisent) and supplemented with 10% FCS (Wisent), at 37°C and 5% CO₂. For 6-well or 12-well plates, 6×10⁵ cells/well or 2×10⁵ cells/well were seeded, respectively, and 24 h later, transiently transfected with 2 μg DNA per 4 μl polyethylenimine (PEI) or 1 μg DNA per 2 μl PEI, respectively. For co-transfections, a 5:1 ratio of APP to RHBDL4 was used. 36 h post-transfection, cells were lysed with TNE-lysis buffer (50 mM Tris, pH 7.4, 150 mM NaCl, 2 mM EDTA, 1% NP40, and complete protease inhibitors, Roche) and prepared for SDS-polyacrylamide gel electrophoresis (SDS-PAGE). 6× SDS sample buffer (2 M Tris/HCl pH 6.8, 20% SDS, 100% glycerol, bromophenol blue, 10% β-mercaptoethanol) was added to the samples for a final concentration of 1×.

Inhibitor treatments

20 h or 36 h post-transfection, cells were treated with 2 μM proteasomal inhibitor MG132 for 16 h or 1 μM γ-secretase inhibitor L685,485 (Tocris) for 12 h, respectively. DMSO was used

as vehicle control. Cells were then lysed according to the aforementioned procedure. 4× LDS sample buffer (with 10% β-mercaptoethanol, Invitrogen) was added to the lysates for a final concentration of 1×.

Western blot and data analysis

Samples were separated on 10% (for NTFs) and 15% (for CTFs) tris-glycine gels by SDS-PAGE. Proteins were transferred onto nitrocellulose membranes with transfer buffer containing 10% ethanol. The following primary antibodies were used: 22C11 (Millipore), 6E10 (Covance), C1/6.1 (Biolegend), anti-RHBDD1 (Sigma), mouse-anti-myc (9B11, Cell Signaling), mouse-anti-β-actin (8H10D10, Cell Signaling), rabbit-anti-Flag (D6W5B, cell signaling). Horseradish peroxidase (HRP)-coupled secondary antibodies directed against mouse or rabbit IgG were purchased from Promega. Chemiluminescent images were acquired using the ImageQuant LAS 500 or 600 system (GE Healthcare).

Acknowledgements

We thank Dr. Claus Pietrzik for kindly providing plasmid cDNAs. This research was supported by grants to L.M.M. by NSERC Discovery grant no. RGPIN-2015-04645, Canada Foundation of Innovation Leaders Opportunity Fund (CFI-LOF, 32565), Alzheimer Society of Canada Young Investigator award PT-58872 and Research Grant 17-02, Fonds d'innovation Pfizer-FRQS sur la maladie d'Alzheimer et les maladies apparentées no. 31288, McGill Faculty of Medicine Incentive funding and an award from The Scottish Rite Charitable Foundation of Canada. S.J.R. received a NSERC USRA summer student stipend.

References

- Adrain, C., Zettl, M., Christova, Y., Taylor, N. and Freeman, M. (2012). Tumor necrosis factor signaling requires iRhom2 to promote trafficking and activation of TACE. *Science* 335, 225-228.
- Arutyunova, E., Panwar, P., Skiba, P., Gale, N., Mak, M. and Lemieux, M. (2014). Allosteric regulation of rhomboid intramembrane proteolysis. *EMBO J.*
- Bhattacharyya, R., Barren, C. and Kovacs, D.M. (2013). Palmitoylation of amyloid precursor protein regulates amyloidogenic processing in lipid rafts. *J Neurosci.* 33, 11169-11183.
- Bonifacino, J.S., Suzuki, C.K. and Klausner, R.D. (1990). A peptide sequence confers retention and rapid degradation in the endoplasmic reticulum. *Science* 247, 79-82.
- Cheng, T.L., Lai, C.H., Jiang, S.J., Hung, J.H., Liu, S.K., Chang, B.I., Shi, G.Y. and Wu, H.L. (2014). RHBDL2 is a critical membrane protease for anoikis resistance in human malignant epithelial cells. *Sci. World J.* 2014, 902987.
- Christova, Y., Adrain, C., Bambrough, P., Ibrahim, A. and Freeman, M. (2013). Mammalian iRhoms have distinct physiological functions including an essential role in TACE regulation. *EMBO Rep.* 14, 884-890.
- De Strooper, B. and Annaert, W. (2000). Proteolytic processing and cell biological functions of the amyloid precursor protein. *J Cell Sci.* 113, 1857-1870.
- El Ayadi, A., Stieren, E., Barral, J. and Boehning, D. (2012). Ubiquilin-1 regulates amyloid precursor protein maturation and degradation by stimulating K63-linked polyubiquitination of lysine 688. *Proc Natl Acad Sci USA* 109, 13416-13421.
- Fleig, L., Bergbold, N., Sahasrabudhe, P., Geiger, B., Kaltak, L. and Lemberg, M.K. (2012). Ubiquitin-dependent intramembrane rhomboid protease promotes ERAD of membrane proteins. *Mol. Cell* 47, 558-569.
- Johnson, N., Brezinova, J., Stephens, E., Burbridge, E., Freeman, M., Adrain, C. and Strisovsky, K. (2017). Quantitative proteomics screen identifies a substrate repertoire of rhomboid protease RHBDL2 in human cells and implicates it in epithelial homeostasis. *Sci. Rep.* 7, 7283.
- Kaden, D., Munter, L., Reif, B. and Multhaup, G. (2012). The amyloid precursor protein and its homologues: structural and functional aspects of native and pathogenic oligomerization. *Eur. J. Cell Biol.* 91, 234-239.
- Kinch, L.N. and Grishin, N.V. (2013). Bioinformatics perspective on rhomboid intramembrane protease evolution and function. *Biochim. Biophys. Acta* 1828, 2937-2943.
- Lemberg, M. and Freeman, M. (2007a). Functional and evolutionary implications of enhanced genomic analysis of rhomboid intramembrane proteases. *Genome Res.* 17, 1634-1646.
- Lemberg, M.K. and Adrain, C. (2016). Inactive rhomboid proteins: new mechanisms with implications in health and disease. *Semin. Cell Dev. Biol.* 60, 29-37.
- Lemberg, M.K. and Freeman, M. (2007b). Cutting proteins within lipid bilayers: rhomboid structure and mechanism. *Mol. Cell* 28, 930-940.

- Lemberg, M.K. and Freeman, M. (2007c). Functional and evolutionary implications of enhanced genomic analysis of rhomboid intramembrane proteases. *Genome Res.* *17*, 1634-1646.
- Lemieux, M.J., Fischer, S.J., Cherney, M.M., Bateman, K.S. and James, M.N. (2007). The crystal structure of the rhomboid peptidase from *Haemophilus influenzae* provides insight into intramembrane proteolysis. *Proc. Natl. Acad. Sci. USA* *104*, 750-754.
- Marrosu, M.G., Vaccargiu, S., Marrosu, G., Vannelli, A., Cianchetti, C. and Muntoni, F. (1998). Charcot-Marie-Tooth disease type 2 associated with mutation of the myelin protein zero gene. *Neurology* *50*, 1397-1401.
- McIlwain, D.R., Lang, P.A., Maretzky, T., Hamada, K., Ohishi, K., Maney, S.K., Berger, T., Murthy, A., Duncan, G., Xu, H.C., Lang, K.S., Haussinger, D., Wakeham, A., Itie-Youten, A., Khokha, R., Ohashi, P.S., Blobel, C.P. and Mak, T.W. (2012). iRhom2 regulation of TACE controls TNF-mediated protection against *Listeria* and responses to LPS. *Science* *335*, 229-232.
- Miao, F., Zhang, M., Zhao, Y., Li, X., Yao, R., Wu, F., Huang, R., Li, K., Miao, S., Ma, C., Ju, H., Song, W. and Wang, L. (2017). RHBDL1 upregulates EGFR via the AP-1 pathway in colorectal cancer. *Oncotarget* *8*, 25251-25260.
- Minopoli, G., de Candia, P., Bonetti, A., Faraonio, R., Zambrano, N. and Russo, T. (2001). The beta-amyloid precursor protein functions as a cytosolic anchoring site that prevents Fe65 nuclear translocation. *J. Biol. Chem.* *276*, 6545-6550.
- Muller, U.C., Deller, T. and Korte, M. (2017). Not just amyloid: physiological functions of the amyloid precursor protein family. *Nat. Rev. Neurosci.* *18*, 281-298.
- Numakura, C., Lin, C.Q., Ikegami, T., Guldberg, P. and Hayasaka, K. (2002). Molecular analysis in Japanese patients with Charcot-Marie-Tooth disease: DGGE analysis for PMP22, MPZ, and Cx32/GJB1 mutations. *Hum. Mutat.* *20*, 392-398.
- Paschkowsky, S., Hamze, M., Oestereich, F. and Munter, L.M. (2016). Alternative processing of the amyloid precursor protein family by rhomboid protease RHBDL4. *J. Biol. Chem.* *291*, 21903-21912.
- Paschkowsky, S., Oestereich, F. and Munter, L.M. (2017). Embedded in the membrane: how lipids confer activity and specificity to intramembrane proteases. *J. Membr. Biol.*
- Reinhard, C., Hebert, S.S. and De Strooper, B. (2005). The amyloid-beta precursor protein: integrating structure with biological function. *EMBO J.* *24*, 3996-4006.
- Shi, G., Lee, J.R., Grimes, D.A., Racacho, L., Ye, D., Yang, H., Ross, O.A., Farrer, M., McQuibban, G.A. and Bulman, D.E. (2011). Functional alteration of PARL contributes to mitochondrial dysregulation in Parkinson's disease. *Hum. Mol. Genet.* *20*, 1966-1974.
- Song, W., Liu, W., Zhao, H., Li, S., Guan, X., Ying, J., Zhang, Y., Miao, F., Zhang, M., Ren, X., Li, X., Wu, F., Zhao, Y., Tian, Y., Wu, W., Fu, J., Liang, J., Wu, W., Liu, C., Yu, J., Zong, S., Miao, S., Zhang, X. and Wang, L. (2015). Rhomboid domain containing 1 promotes colorectal cancer growth through activation of the EGFR signalling pathway. *Nat. Commun.* *6*, 8022.
- Stangeland, B., Mughal, A.A., Grieg, Z., Sandberg, C.J., Joel, M., Nygard, S., Meling, T., Murrell, W., Vik Mo, E.O. and Langmoen, I.A. (2015). Combined expressional analysis, bioinformatics and targeted proteomics identify new potential therapeutic targets in glioblastoma stem cells. *Oncotarget* *6*, 26192-26215.

- Strisovsky, K. (2016). Why cells need intramembrane proteases – a mechanistic perspective. *FEBS J.* 283, 1837-1845.
- Strisovsky, K. and Freeman, M. (2014). Sharpening rhomboid specificity by dimerisation and allostery. *EMBO J.* 33, 1847-1848.
- Strisovsky, K., Sharpe, H.J. and Freeman, M. (2009). Sequence-specific intramembrane proteolysis: identification of a recognition motif in rhomboid substrates. *Mol Cell* 36, 1048-1059.
- Ulmschneider, M.B., Ulmschneider, J.P., Freites, J.A., von Heijne, G., Tobias, D.J. and White, S.H. (2017). Transmembrane helices containing a charged arginine are thermodynamically stable. *Eur. Biophys. J.* 46, 627-637.
- Urban, S. and Baker, R.P. (2008). *In vivo* analysis reveals substrate-gating mutants of a rhomboid intramembrane protease display increased activity in living cells. *Biol. Chem.* 389, 1107-1115.
- Urban, S. and Freeman, M. (2003). Substrate specificity of rhomboid intramembrane proteases is governed by helix-breaking residues in the substrate transmembrane domain. *Mol. Cell* 11, 1425-1434.
- Urban, S., Lee, J.R. and Freeman, M. (2001). Drosophila rhomboid-1 defines a family of putative intramembrane serine proteases. *Cell* 107, 173-182.
- Walder, K., Kerr-Bayles, L., Civitarese, A., Jowett, J., Curran, J., Elliott, K., Trevaskis, J., Bishara, N., Zimmet, P., Mandarino, L., Ravussin, E., Blangero, J., Kissebah, A. and Collier, G.R. (2005). The mitochondrial rhomboid protease PSARL is a new candidate gene for type 2 diabetes. *Diabetologia* 48, 459-468.
- Wang, Y., Zhang, Y. and Ha, Y. (2006). Crystal structure of a rhomboid family intramembrane protease. *Nature* 444, 179-180.
- Wolfe, M.S. (2012). Processive proteolysis by gamma-secretase and the mechanism of Alzheimer's disease. *Biol. Chem.* 393, 899-905.
- Wunderle, L., Knopf, J.D., Kuhnle, N., Morle, A., Hehn, B., Adrain, C., Strisovsky, K., Freeman, M. and Lemberg, M.K. (2016). Rhomboid intramembrane protease RHBDL4 triggers ER-export and non-canonical secretion of membrane-anchored TGF α . *Sci. Rep.* 6, 27342.

Figure legends

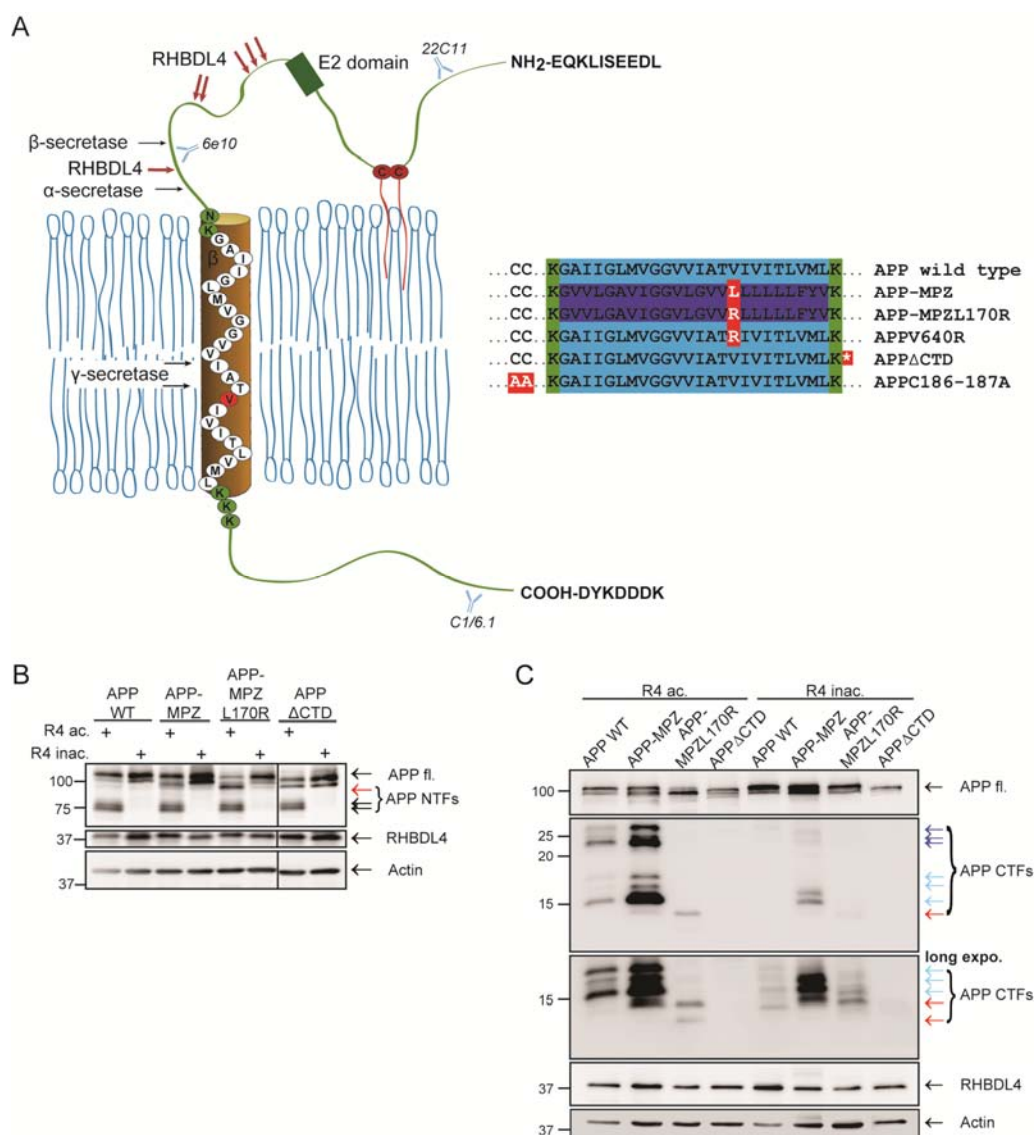


Figure 1 RHBDL4 exhibits a dual cleavage mode mechanism.

(A) Schematic of APP wild type (WT) with detailed transmembrane sequence and indicated cysteines residues at position 186 and 187 in the ectodomain, encircled in red. Black arrows indicate cleavage sites of canonical proteases involved in APP processing while red arrows point to RHBDL4 cleavage sites reported in Paschkowsky *et al.* (2016). Furthermore, shown on the right is a partial amino acid sequence of APP encompassing mutations in transmembrane region, ectodomain or deletion of the cytoplasmic tail. Antibodies used in this study are indicated in the schematic. All constructs express a C-terminal Flag and N-terminal Myc tag. (B) Analysis of full-length APP (APP fl.) and N-terminal fragments (APP NTFs) in HEK 293T cells co-expressing active (R4 ac.) or inactive RHBDL4 (R4 inac.). APP wild

Novel bimodal cleavage pattern of RHBDL4

type, chimeric mutants (APP-MPZ and MPZ L170R) or APP lacking the C-terminal domain (APP Δ CTD) co-expressed with RHBDL4 show a reduction in APP fl. levels and occurrence of 70-73 kDa NTFs (black arrows). Red arrow indicates a novel RHBDL4-specific larger NTF. APP full-length and NTFs were detected with 22C11, RHBDL4 was stained with anti-RHBDL4 and β -actin was used as loading control. Shown is a representative western blot of three independent experiments. (C) Comparison of RHBDL4-derived APP CTF pattern between WT and different variants. All CTFs derived from overexpression of an APP construct are labelled with anti-Flag antibody (2nd and 3rd panel). Detection of APP fl by 6E10 antibody. Co-expression of APP wild type and APP-MPZ with active RHBDL4 generated 15-27 kDa CTFs (indicated by dark and light blue arrows), red arrow indicates a novel smaller fragment for APP-MPZL170R. RHBDL4 was detected with anti-flag; β -actin was used as loading control. Shown is a representative western blot of three independent experiments.

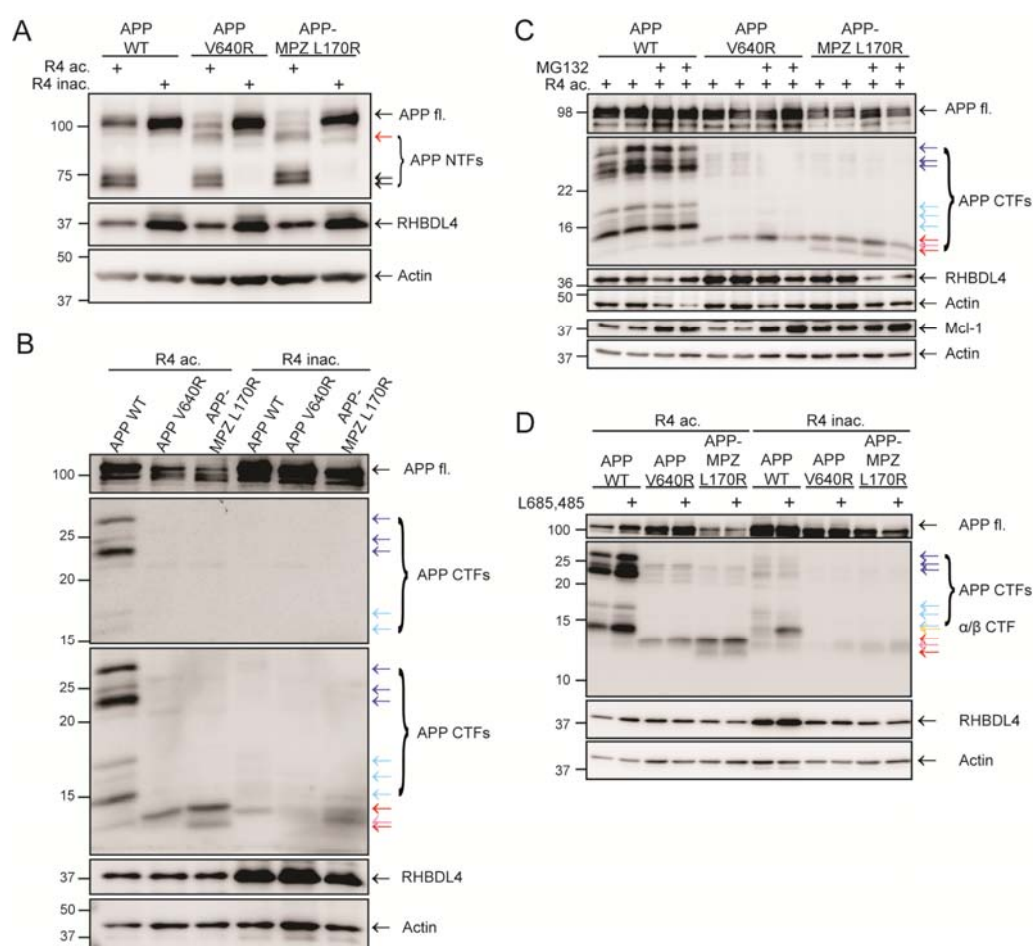


Figure 2 The substrate transmembrane sequence confers different cleavage modes of RHBDL4.

Novel bimodal cleavage pattern of RHBDL4

(A) Co-transfection of APP wild type, APP V640R or APP-MPZ L170R together with active or inactive RHBDL4 in HEK 293T cells. APP fl and 70-73 kDa NTFs are indicated by black arrows; novel large NTF is indicated by a red arrow (detection with 22C11). RHBDL4 was stained with anti-RHBDL4; β -actin was used as loading control. Shown is a representative western blot of four independent experiments. (B) Analysis of RHBDL4-specific CTF cleavage pattern. Co-expression of RHBDL4 active and inactive together with APP wild type, APP V640R or APP-MPZL170R. Dark and light blue arrows indicate previously published RHBDL4-derived 15-27 kDa CTFs. Red arrows indicate RHBDL4-specific smaller CTFs that are C1/6.1- but not 6E10-reactive. Pink arrow indicates an additional smaller fragment that was only detected for WT and ran likely between the two CTFs generated from the APP variants. APP fl labelled with C1/6.1, RHBDL4 detected with anti-RHBDL4 and β -actin used as loading control. Shown is a representative Western blot of four independent experiments. (C) 30 h post transfection cells co-expressing APP variants and RHBDL4 were treated with MG132 for 16 h. As expected, treatment increased Mcl-1 levels in all samples. No effect on 15-27 kDa RHBDL4-specific CTFs (indicated by dark and light blue arrows) was observed; however, novel C1/6.1-reactive CTFs (indicated by red arrows) accumulated upon proteasome inhibition. APP fl labelled with C1/6.1, RHBDL4 detected with anti-RHBDL4 and β -actin used as loading control. Shown is a representative western blot of three independent experiments. (D) HEK 293T cells co-expressing RHBDL4 and APP variants were treated for 12h with a γ -secretase inhibitor (L685,485). Accumulation of α/β -CTF (indicated by a yellow arrow) but no effect on RHBDL4-derived CTFs was observed. APP fl and CTFs detected with C1/6.1, RHBDL4 stained with anti-flag; β -actin used as loading control. Shown is a representative western blot of four independent experiments.

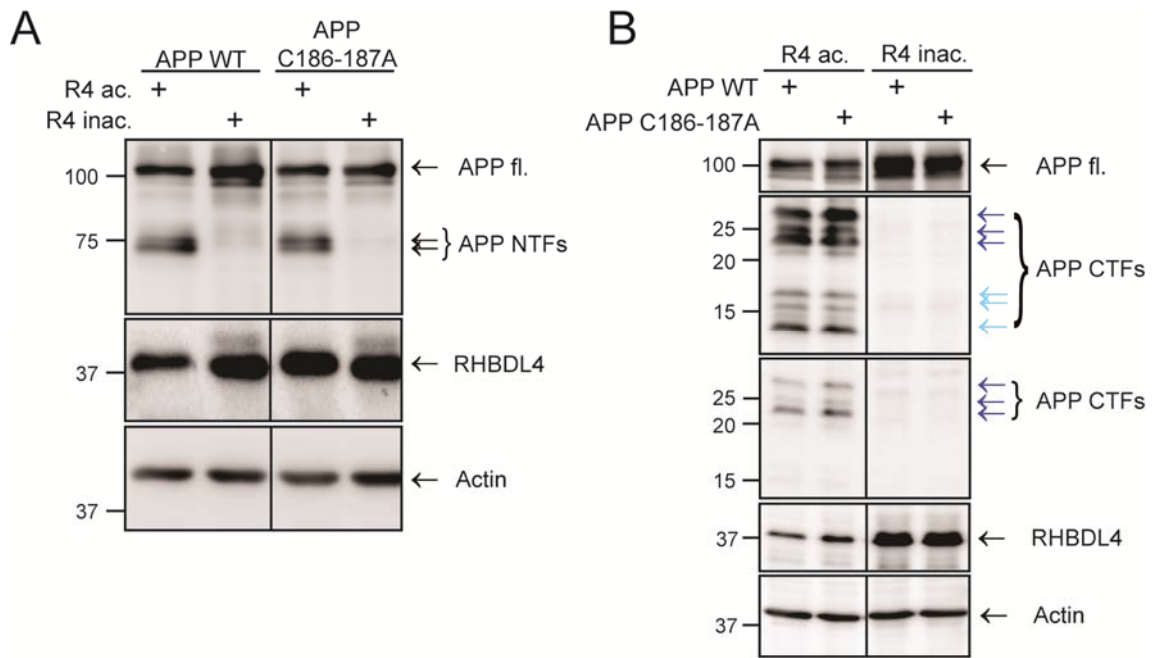


Figure 3 Cysteine mutants do not affect RHBDL4-mediated ectodomain cleavages of APP.

(A) Upon co-expression of APP C186-187A with active RHBDL4, similar NTFs as compared to WT and reduced APP fl were detected with 22C11. RHBDL4 stained with anti-flag; β -actin used as loading control. Shown is a representative western blot of three independent experiments. (B) Co-expression of RHBDL4 active and APP C186-187A resulted in the generation of 15-27 kDa CTFs, similar to WT. RHBDL4-specific large CTFs were labelled using 6E10 (panel 3) and C1/6.1 stained large and small CTFs (panel 2; dark and light blue arrows, respectively). Detection of RHBDL4 with anti-RHBDL4; β -actin used as loading control. Shown is a representative western blot of three independent experiments.